Metrology at the ingot level: Addressing the growing importance of bulk material quality

Bernhard Mitchell[1], **Daniel Chung**[1], **Jürgen Weber**[2] & **Thorsten Trupke**[1,2]

[1]University of New South Wales (UNSW), Sydney; [2]BT Imaging Pty Ltd, Sydney, Australia

ABSTRACT

With the PV industry continually pushing for ever-higher silicon solar cell efficiencies, the requirements on the electronic quality of the bulk material are becoming more stringent. Advanced characterization of silicon ingots after cutting into bricks allows early quality control and immediate feedback in crystal growth, thereby facilitating shorter R&D cycles, higher yield, lower cost and higher product quality in mass manufacturing. Techniques based on photoluminescence (PL) imaging for bricks and ingots have been developed and refined over the last few years and now provide crucial material parameters, such as the bulk minority-carrier lifetime, in a quick and reliable fashion. In this paper some of these quantitative methods, which are already available in commercial inspection tools, are demonstrated on state-of-the-art industrial high-performance multicrystalline p-type Si bricks and high-lifetime n-type Cz-Si ingots.

The case for ingot-level metrology

The rapid improvement in industrial solar cell manufacturing over the last ten years in terms of average conversion efficiencies and cost reduction is nothing short of spectacular. SunPower recently presented statistical manufacturing data for their latest generation of high-efficiency solar cells, with average efficiencies exceeding 24%, and for even a full-size module an aperture efficiency of 24.1% [1]. Trina recently reported record efficiencies for passivated emitter rear cells (PERCs) on both six-inch mono- and multicrystalline Si wafers [2,3]. With most solar cell manufacturers, higher-efficiency PERC solar cells are in either full-scale or pilot production, while others are focusing on alternative high-efficiency solar cell concepts, such as heterojunction solar cells. These trends towards ever-increasing efficiency in production are expected to continue for many years, particularly in the case of the more conventional cell architectures.

> "The inspection of silicon ingots and bricks represents the only opportunity to reliably measure the bulk lifetime at an early processing stage."

Ultimately, the performance of a solar cell is determined by a number of loss mechanisms. For screen-printed full-area Al-BSF solar cells, still currently the industry standard, the loss mechanisms which are related to the device design, such as recombination at the rear metal surface, dominate and limit cell performance. In advanced cell designs these unwanted processing-related or device-architecture-related recombination sources are significantly reduced or eliminated. As a result, the bulk quality of the Si wafer itself becomes an increasingly significant factor. A key parameter representing the electronic absorber quality is the bulk excess minority-carrier lifetime τ_b, or short bulk lifetime, which defines how long photogenerated excess carriers (electron–hole pairs) 'survive' within the absorber before they recombine. A higher bulk lifetime yields higher cell voltages and higher currents, and thus higher efficiency. The inspection of silicon ingots and bricks represents the only opportunity to reliably measure the bulk lifetime at an early processing stage, since that information is largely lost during wafer cutting, the lifetime in as-cut wafers being severely limited by surface recombination.

In crystalline Si, τ_b is found to be mostly determined by contaminants, such as transition metals, light elements (O, C, N) and imperfections in the crystal lattice (micro and extended defects). Multicrystalline Si ingots grown by directional solidification (DS) exhibit extended defects, such as grain boundaries and dislocation clusters; the latter are often contaminated by precipitates or dissolved point defects. As-grown bulk lifetimes vary considerably throughout cast ingots and depend on a wide range of parameters, such as the purity of the feedstock, the type of crucible and lining, and, of course, the growth conditions (e.g. temperature profiles) during crystallization. Intra-grain lifetimes reaching several hundred microseconds can be achieved in both boron-doped and phosphorus-doped high-performance multicrystalline (HPM) Si ingots, and can be further greatly improved by diffusion-assisted gettering [4,5].

Czochralski (Cz)-grown ingots do not usually show extended defects, but are affected by grown-in micro or point defects (voids, oxygen precipitates, etc.) and contaminants (e.g. carbon [6]), which affect the bulk lifetime. The as-grown bulk lifetimes of Cz crystals are higher than in the case of DS-grown ingots (up to tens of milliseconds). In p-type Cz-Si, the bulk lifetime is often limited by recombination via boron–oxygen complexes [7].

The early measurement of the bulk lifetime and other defect parameters at the ingot level can add significant value in terms of maximizing efficiency and yield in production – for example via: 1) immediate feedback to crystal growth; 2) discarding of unsuitable material at an early stage; 3) classification of wafer material; and 4) sorting of bricks and wafers for selective processing.

Specifically in relation to the first

point above, ingot-level metrology enables faster R&D cycles and can be used, for example, to improve throughput, reduce the dislocation density in DS cast ingots, develop and evaluate new seeding techniques, track metal contamination, test new crucibles and lining materials, improve homogeneity across the crystal, and trace thermal donor growth. Without comprehensive ingot metrology, feedback from the above activities usually requires cell processing, which involves the entire solar cell production sequence, including wafer cutting, cell processing and careful tracking of these activities. Not only is this process time consuming, but it is also prone to errors and demands significant resources.

Spectral PL imaging: a rapid quantitative bulk lifetime technique

Techniques available for the characterization of Si ingots and bricks in mass manufacturing include microwave-detected photoconductance decay (PCD) and quasi-steady-state photoconductance (QSSPC). Both of these have specific shortcomings when applied to non-passivated bricks.

PCD measures and reports significantly surface-limited *effective* lifetimes only; in addition, these values are reported at high injection levels ($>1\times10^{15}cm^{-3}$), which are not representative of the typical operation of solar cells. Measurement times of several minutes are normally required in order to obtain a relatively coarse spatially resolved map (e.g. 2mm raster scan) of effective lifetime. QSSPC, or eddy-current-detected PCD, measurements can provide *true* bulk lifetime at the ingot level, but yield only very limited spatial resolution of the order of centimetres, which does not allow the detection and quantification of structural defect densities. Both PCD and QSSPC techniques can be affected (in some cases severely) by trapping artefacts, which can prevent a reliable bulk lifetime analysis at the injection levels relevant to solar cell operation [8,9].

Photoluminescence (PL) imaging provides a powerful alternative to the above techniques. Over the last few years, a range of quantitative analysis techniques for the application of PL imaging at the ingot level have been developed at UNSW, which have now matured to a level that makes them suitable for implementation in commercial tools. One particularly successful development is the quantitative analysis of the emission spectrum. The PL spectrum of a thick sample, e.g. a Si brick or thick Si disc, contains significant bulk lifetime information. This information can be extracted using the so-called *spectral PL intensity ratio (sPLIR)* method, which involves imaging the sample twice, with two different spectral filters mounted in front of the camera lens. The two different filters change the sensing depth of the PL detection, enabling signals to be captured that relate to the carrier density at different depths within the brick. The theory behind this technique, which was first proposed by Würfel [10] for the characterization of the diffusion length in fully processed silicon solar cells, is described in detail elsewhere [11,12]. Importantly, the technique enables the acquisition of high-resolution (approximately 150µm per pixel) bulk lifetime images on bricks of any length (BT Imaging LIS-B3 system – up to 40cm), with total acquisition times of less than one minute; the method is also insensitive to variations in bulk resistivity.

> "In unpassivated bricks the sPLIR technique is sensitive to bulk lifetime variations from a few microseconds to tens of milliseconds."

Another key strength of this technique is that it works for a very broad range of diffusion lengths, from approximately 10µm to 10mm, as shown in Fig. 1. The equivalent excess minority-carrier lifetime range for p-type material is shown on the top axis for comparison; according to this, in unpassivated bricks the sPLIR technique is sensitive to bulk lifetime variations from a few microseconds to tens of milliseconds, thus covering the entire range relevant to PV applications.

According to the theoretical analysis carried out, the use of Si cameras (as opposed to, for example, InGaAs cameras) has inherent benefits for the sPLIR application, specifically because of a better sensitivity to lifetime variations at low lifetimes, as typically found near the top and bottom sections of mc-Si ingots [13]. On the other hand, PL imaging applications using Si area cameras suffer from image blurring, which is caused by the poor absorption of Si luminescence photons [13–15] and the resulting lateral scattering within the CCD chip. As recently demonstrated [16], this experimental artefact is greatly suppressed when using line-scanning PL imaging rather than conventional area-scanning cameras, resulting in significantly improved accuracy of the method. By means of the line-scanning principle, ingots of virtually any length can be measured conveniently without the need to stitch individual images together.

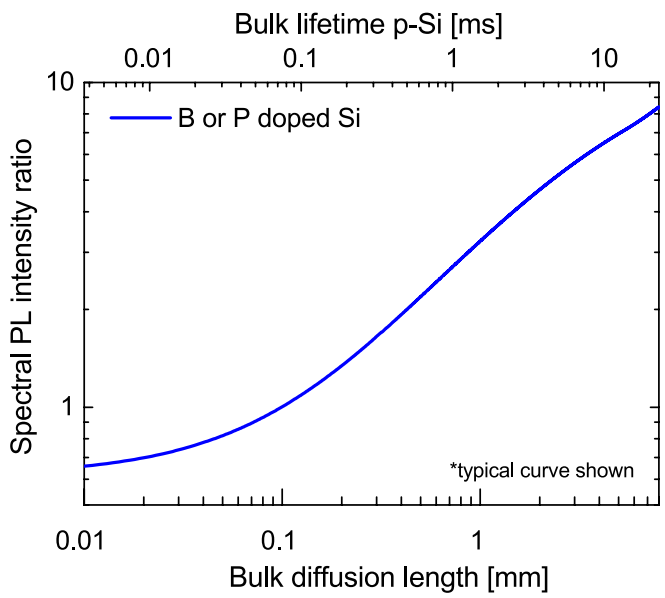

Figure 1. Theoretical dependence of the sPLIR signal on the excess minority-carrier bulk diffusion length for an unpassivated and infinitely thick Si block. The top axis represents the equivalent excess minority-carrier bulk lifetime for p-type silicon.

Bulk lifetime and iron concentration: two key bulk material quality parameters

The sPLIR technique has been applied to and verified on a broad range of samples. Fig. 2(a) shows a bulk lifetime image of a state-of-the-art HPM boron-doped Si brick from a G6 furnace (data measured on a BT Imaging LIS-B3 system). Significant variations in bulk lifetime are observed, with values ranging from less than 1µs to 140µs. The impact of structural defects, such as decorated grain boundaries and dislocation clusters, is also visible.

An example of the bulk lifetime from sPLIR imaging of a high-lifetime n-type Cz-grown ingot is shown in Fig. 2(b). A severe degradation in bulk lifetime because of oxygen-induced stacking faults is observed across a large portion of the brick. Lifetime values of up to 6ms are observed in the 'good' regions of the ingot, demonstrating the wide dynamic range of detectable lifetimes.

When applied to the outside surfaces of bricks and ingots, the sPLIR approach provides bulk lifetime information for only the first few millimetres from the surface. In order to characterize lifetime variations within an ingot, the sPLIR method can be carried out either on specially prepared vertical slabs [17] or on thick discs that have been cut in the wafer plane (see example in Fig. 2(c)). Up to 20ms lifetimes on a 2cm-thick high-lifetime n-type disc were recently measured, demonstrating the ability to measure extremely high lifetimes on non-passivated samples (data submitted for publication elsewhere).

Iron is a detrimental impurity in boron-doped Si [18] and arguably one of the dominant sources of recombination in DS-Si ingots because of the diffusion of impurities from the crucible and the lining [19,20], in addition to sources in the feedstock (cf. Fig. 4(c)). Iron is typically found around the entire perimeter (top, bottom and side faces) of DS-cast ingots, as a result of in-diffusion, segregation and solid-state back diffusion during cooling. Iron can be present in either precipitated or dissolved states in DS mc-Si, while it is usually found only in the dissolved state in Cz-Si. The edge regions of a DS ingot contain both

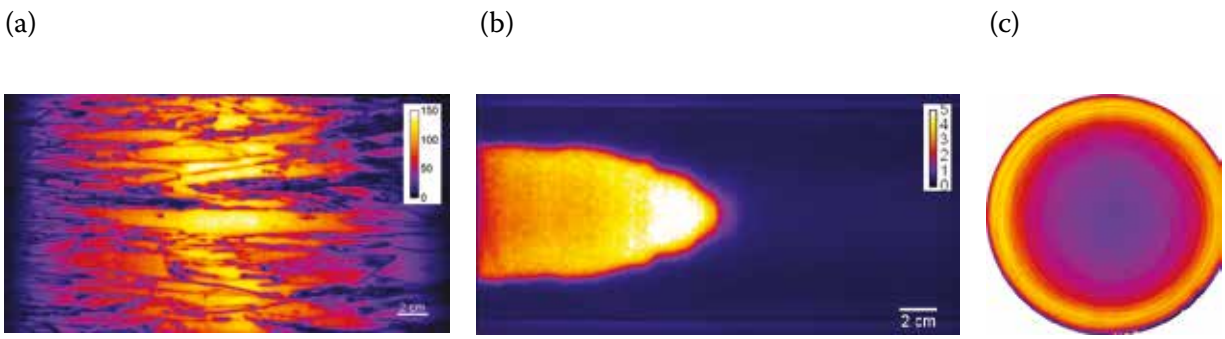

Figure 2. sPLIR bulk lifetime images for (a) a p-type HPM brick (scale in µs) and (b) an n-type Cz-Si brick (scale in ms). (c) Raw sPLIR image of an n-type Cz-Si disc sawn from near the crown of the ingot. All samples were measured without surface passivation (data from a BT Imaging LIS-B3 system).

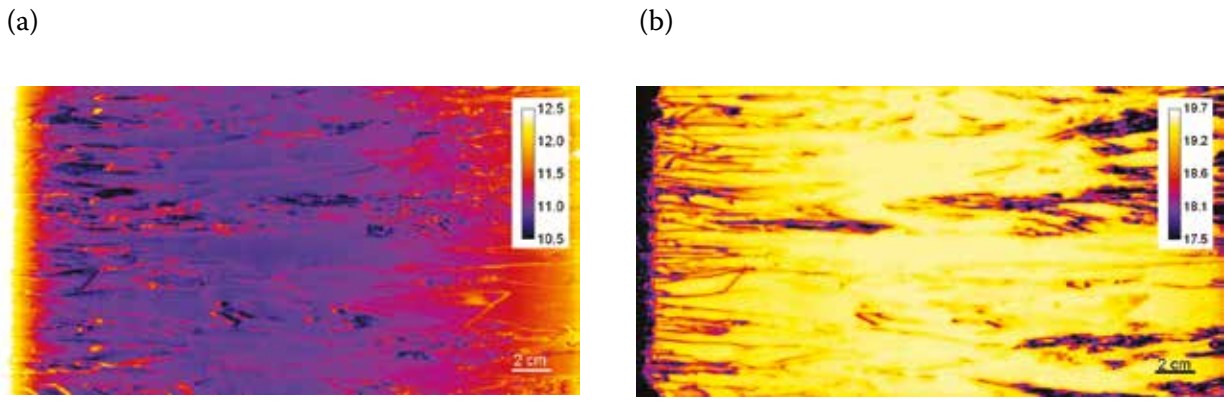

Figure 3. (a) Dissolved iron concentration on a logarithmic scale (in cm^{-3}) for an HPM brick. (b) Predicted solar cell efficiency image (in %) of the same HPM brick (see text for details). Cell efficiencies would vary by about $0.6\%_{abs}$ as a function of ingot height, if as-grown background lifetime were used as a predictive measure of cell performance.

dissolved and precipitated iron, but the recombination in the centre of the ingot is mostly due to dissolved (either interstitial or FeB) iron, though nanoscale precipitates may exist in the as-grown state or are induced through cell processing [21].

Given its ability to measure spatially resolved bulk lifetime, the sPLIR imaging method also allows quantitative measurement of the dissolved iron concentration in *boron-doped* Si bricks or discs (either DS or Cz). In this approach an intense light source is used to toggle the dissolved iron between interstitial and FeB states, the latter being the equilibrium state in silicon at room temperature [22,23]. The variation in bulk lifetime resulting from the dissociation of FeB pairs can be linked quantitatively to the iron concentration. The method therefore includes the sequence of a first bulk lifetime image from sPLIR, followed by the dissociation of the FeB pairs using a flash lamp, and then a second bulk lifetime image. This technique was applied to the HPM block shown in Fig. 2(a). Fig. 3(a) shows the extracted dissolved iron concentration across the same brick face (bottom of the ingot is shown on the left). Low interstitial iron concentrations of the order of 5×10^{10}cm^{-3} were measured in the central high-lifetime region, whereas high concentrations up to 1×10^{13}cm^{-3} were observed in the low-lifetime bottom region; in the latter region, the iron dominates the total recombination and is the main cause of the reduction in bulk lifetime reported in Fig. 3(a).

> "The sPLIR imaging method also allows quantitative measurement of the dissolved iron concentration in *boron-doped* Si bricks or discs."

Beyond pure contamination screening, the additional information about iron concentration can be used to define performance classes for as-grown wafer material. For example, with the knowledge of the as-grown bulk lifetime and the as-grown dissolved iron concentration, it is possible to predict the background lifetime, in other words the bulk lifetime that would be present and measured in the absence of dissolved iron. The *background lifetime* is expected to be more useful for predicting the bulk quality in the final device than the as-grown bulk lifetime, since many conventional cell processes include a phosphorus diffusion, which represents an efficient gettering process that reduces the iron concentration in the bulk.

Combined with a cell performance curve (CPC) for a specific device concept, which can be obtained from detailed device simulations, it is thus possible to rate silicon material in terms of expected solar cell performance, entirely on the basis of ingot measurements using sPLIR imaging. Note that the degree of applicability of this hypothesis is currently being investigated experimentally in collaboration with industry partners, and is dependent on the exact cell processing conditions, and thus on cell architecture. The analysis here was performed on the HPM sample from Fig. 2(a). The resulting 'predicted efficiency' image (Fig. 3(b)) shows a variation of 0.6%$_{abs}$ across the ingot height; this spread is associated with just the variations in bulk lifetime. These predicted efficiency variations therefore do not account for the extended defect density variation.

Material quality variations in production

The above methods were applied to industrial bricks manufactured in the last few years, and significant variations were found in the material quality within ingots, across different batches and manufacturers and with time. As an example, Fig. 4 compares the bulk lifetime, iron concentration and interstitial iron recombination fraction (i.e. the percentage of the iron-related recombination of total recombination) for four industrial bricks. The sample set consists of two standard mc-Si bricks manufactured in 2011, and two recent HPM bricks (for details see Chung et al. [24]).

It was found that current HPM ingots tend to yield slightly higher bulk lifetimes than traditionally produced ingots from a few years ago, but can show vastly different height distributions (see HPM1 vs. HPM2). With regard to the dissolved iron profiles, all bricks show qualitatively similar profiles, with no obvious differential trend between the conventional bricks and HPM

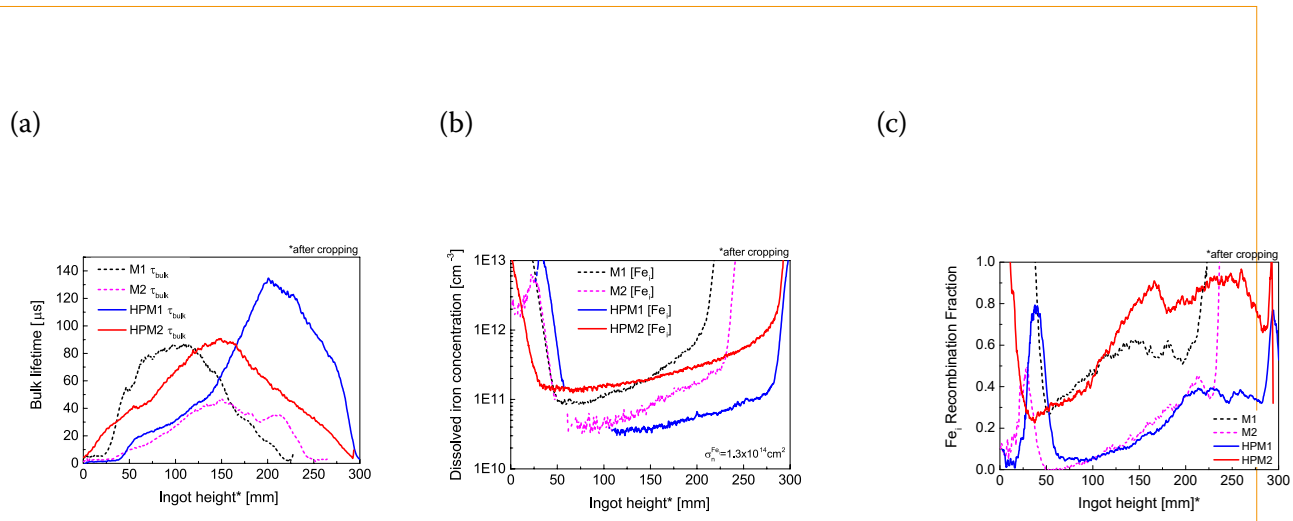

Figure 4. (a) Bulk lifetime, (b) dissolved iron, and (c) dissolved iron recombination fraction as a function of ingot height, for a set of four industrial DS ingots (two standard mc, two HPM).

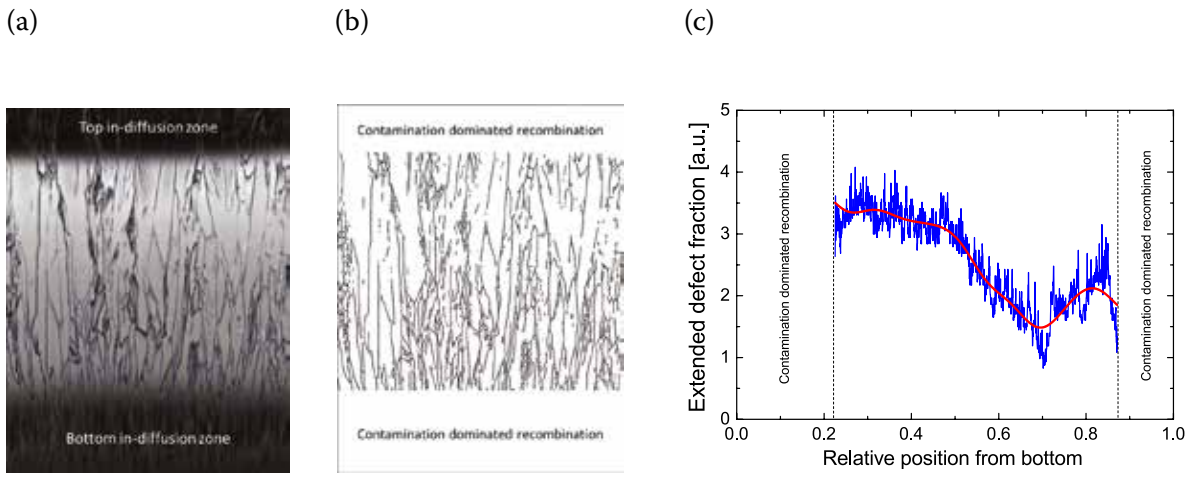

Figure 5. (a) PL image of a HPM Si brick. (b) Extended defect structure detected using PL imaging. (c) Height dependence of extended defects.

bricks, but quantitative differences are noteworthy and may lead to valuable insight when measured in dependency of crucible, lining and/or feedstock quality and the crystallization recipe. Note that HPM1 demonstrates a significantly lower value than HPM2, even though the bulk lifetimes are not necessarily higher. This is reflected in the fact that HPM1 is less strongly dominated by dissolved iron than HPM2. Other defects must play a role in HPM1, which is powerful information to have in manufacturing, when results from cell production and other characterization are available. Overall, the recombination fraction profiles show that, for most of the bricks, interstitial iron is a dominant lifetime-limiting factor in the as-grown material. Its influence increases towards the top of the brick, where dissolved iron is known to decorate extended defects that are harder to getter effectively. The availability of this quantitative information from a quick and convenient measurement system can obviously be of great value to R&D engineers for further improvement and refinement of the crystallization process.

Extended defect analysis

The major improvement in HPM bricks compared with earlier DS bricks is the significant reduction in structural defects, particularly in the density of dislocation clusters; these have been shown in several studies [25,26] to have a strong and dominating effect on the efficiency of mc-Si cells.

The BT Imaging LIS-B3 system provides high spatial resolution and outstanding image quality, allowing various quality metrics that are related to (among other things) the density of the above structural defects to be extracted using automated image processing algorithms. This capability is demonstrated here (see Fig. 5) using a basic feature analysis routine developed at UNSW. The LIS-B3 incorporates and reports more-sophisticated metrics, which evolved from image-processing algorithms developed for commercial PL-imaging-based wafer inspection systems; these have already played an important role in the improvement of mc-Si quality in terms of reducing structural defects to the current levels. When applied at the brick level, the PL imaging analysis and related quantitative metrics can result in even faster process feedback, and will therefore be a valuable tool for further improvements in mc-Si and for process monitoring in high-volume manufacturing.

Conclusions

PL imaging of bricks and ingots using line scanning is an attractive alternative to existing characterization methods currently used in production and in R&D labs. Short measurement times, the non-contact nature, high spatial resolution and robustness against various measurement artefacts are some key advantages. Advanced quantitative analyses in terms of various key material parameters (e.g. *true* bulk lifetime and dissolved iron concentration) are made possible by the application of sophisticated experimental methods, such as the sPLIR method developed at UNSW, which exploits the information about the electronic material quality that is contained in the spectral distribution of the emitted luminescence.

> "PL imaging of bricks and ingots using line scanning is an attractive alternative to existing characterization methods currently used in production and in R&D labs."

The systematic application of those methods in R&D and production, using reliable inspection systems with superior throughput, will contribute to further improvements in crystal quality and yield, and thereby ultimately contribute to the further cost reductions in PV manufacturing that are still required. Immediate applications range from the optimization of crystallization processes via process monitoring in production, to the use of PL images as a cutting guide. In the medium term the bulk lifetime information, which can be reliably extracted from PL images, can also be used to classify the raw material, with the aim of wafer-specific processing in order to maximize the efficiency of the solar cells created from across an ingot.

Acknowledgements

This research has been supported by the Australian Government through the Australian Renewable Energy

Agency (ARENA) grants 7-F008 and RND009. The Australian Government does not accept responsibility for the views, information or advice expressed herein. The authors would like to thank Dr. Oliver Kunz for his contributions.

References

[1] Smith, D.D. et al. 2016, "Silicon solar cells with total area efficiency above 25 %", *Proc. 43rd IEEE PVSC*, Portland, Oregon, USA.

[2] Ye, F. et al. 2016, "22.13 % efficient industrial p-type mono PERC solar cell", *Proc. 43rd IEEE PVSC*, Portland, Oregon, USA.

[3] Zhang, S. et al. 2016, "335-W world-record p-type monocrystalline module with 20.6% efficient PERC solar cells", *IEEE J. Photovolt.*, Vol. 6, No. 1, pp. 145–152.

[4] Schön, J. et al. 2015, "Identification of the most relevant metal impurities in mc n-type silicon for solar cells", *Sol. Energy Mater. Sol. Cells,* pp. 1–9.

[5] Michl, B. et al. 2013, "The impact of different diffusion temperature profiles on iron concentrations and carrier lifetimes in multicrystalline silicon wafers", *IEEE J. Photovolt.*, Vol. 3, No. 2, pp. 635–640.

[6] Nagai, Y. et al. 2016, "Growth of Czochralski silicon crystals having ultralow carbon concentrations", *Gettering Defect Eng. Semicond. Technol. XVI*, Vol. 242, pp. 3–9.

[7] Walter, D.C., Lim, B. & Schmidt, J. 2016, "Realistic efficiency potential of next-generation industrial Czochralski-grown silicon solar cells after deactivation of the boron-oxygen-related defect center", *Prog. Photovoltaics Res. Appl.*, Vol. 24, No. 7, pp. 920–928.

[8] Macdonald, D. & Cuevas, A. 1999, "Trapping of minority carriers in multicrystalline silicon", *Appl. Phys. Lett.,* Vol. 74, No. 12, pp. 1710–1712.

[9] Hu, Y. et al. 2012, "Investigating minority carrier trapping in n-type Cz silicon by transient photoconductance measurements", *J. Appl. Phys.*, Vol. 111, No. 5, pp. 0–6.

[10] Würfel, P. et al. 2007, "Diffusion lengths of silicon solar cells from luminescence images", *J. Appl. Phys.*, Vol. 101, No. 12, p. 123110.

[11] Mitchell, B. et al. 2011, "Bulk minority carrier lifetimes and doping of silicon bricks from photoluminescence intensity ratios", *J. Appl. Phys.*, Vol. 109, No. 8, pp. 083111-1–083111-12.

[12] Green, M.A. 2011, "Analytical expressions for spectral composition of band photoluminescence from silicon wafers and bricks", *Appl. Phys. Lett.,* Vol. 99, No. 13, p. 131112.

[13] Mitchell, B. et al. 2012, "On the method of photoluminescence spectral intensity ratio imaging of silicon bricks: Advances and limitations", *J. Appl. Phys.*, Vol. 112, No. 6, pp. 063116–1–063116–13.

[14] Walter, D. et al. 2012, "Contrast Enhancement of Luminescence Images via Point-Spread Deconvolution", *Proc. 38th IEEE PVSC*, Austin, Texas, USA.

[15] Breitenstein, O., Frühauf, F. & Teal, A. 2016, "An improved method to measure the point spread function of cameras used for electro- and photoluminescence imaging of silicon solar cells", *IEEE J. Photovolt.*, Vol. 60, No. 5, pp. 1–6.

[16] Mitchell, B., Chung, D. & Teal, A. 2016, "Photoluminescence imaging using silicon line-scanning cameras", *IEEE J. Photovolt.,* pp. 1–9.

[17] Hu, Y., Schøn, H. & Arnberg, L. 2013, "Characterization of defect patterns in Cz silicon slabs by carrier density imaging", *J. Cryst. Growth,* Vol. 368, pp. 6–10.

[18] Schmidt, J. et al. 2013, "Impurity-related limitations of next-generation industrial silicon solar cells", *IEEE J. Photovolt.,* Vol. 3, No. 1, pp. 114–118.

[19] Schubert, M.C. et al. 2013, "Impact of impurities from crucible and coating on mc-silicon quality – The example of iron and cobalt", *IEEE J. Photovolt.,* Vol. 3, No. 4, pp. 1250–1258.

[20] Schindler, F. et al. 2014, "Solar cell efficiency losses due to impurities from the crucible in multicrystalline silicon", *IEEE J. Photovolt.*, Vol. 4, No. 1, pp. 122–129.

[21] Kwapil, W. et al. 2014, "Impact of iron precipitates on carrier lifetime in as-grown and phosphorus-gettered multicrystalline silicon wafers in model and experiment", *IEEE J. Photovolt.,* Vol. 4, No. 3, pp. 791–798.

[22] Mitchell, B. et al. 2014, "Imaging as-grown interstitial iron concentration on boron-doped silicon bricks via spectral photoluminescence", *IEEE J. Photovolt.*, Vol. 4, No. 5, pp. 1185–1196.

[23] Macdonald, D., Tan, J. & Trupke, T. 2008, "Imaging interstitial iron concentrations in boron-doped crystalline silicon using photoluminescence", *J. Appl. Phys.,* Vol. 103, No. 7, pp. 073710-1–073710-7.

[24] Chung, D. et al. 2016, "Photoluminescence imaging for quality control in silicon solar cell manufacturing", *MRS Adv.,* June, pp. 1–10.

[25] Haunschild, J. et al. 2010, "Quality control of as-cut multicrystalline silicon wafers using photoluminescence imaging for solar cell production", *Sol. Energy Mater. Sol. Cells*, Vol. 94, No. 12, pp. 6–11.

[26] Demant, M. et al. 2015, "Inline quality rating of multi-crystalline wafers based on photoluminescence images", *Prog. Photovoltaics Res. Appl.,* Vol. 20, No. 1, pp. 1–14.

About the Authors

Bernhard Mitchell is a research fellow at the Australian Centre for Advanced Photovoltaics at UNSW. Since receiving his Ph.D. in 2013 he has led activities involving Si ingot characterization at UNSW. He is a semiconductor physicist with more than 10 years' research experience in the PV sector both in silicon and in III-V technologies.

Daniel Chung is a Ph.D. student at the Australian Centre for Advanced Photovoltaics at UNSW. His research focuses on the development of photoluminescence characterization with regard to silicon ingots and applications in solar cell manufacturing.

Jürgen Weber began his career in PV as an engineer with a measurement technology specialization at the Fraunhofer CalLab in 2000, and subsequently worked at UNSW in the thin-film group and as a characterization laboratory manager. He joined BT Imaging in 2009, where for the last few years he has focused on the development and optimization of line-scanning PL systems.

Thorsten Trupke is a semiconductor physicist having more than 15 years' experience in R&D in the PV sector and specialising in the development of novel characterization methods. He is a professor at the Australian Centre for Advanced Photovoltaics at UNSW, as well as the co-founder and CTO of BT Imaging – a UNSW start-up company that commercializes PL-imaging inspection systems.

Enquiries

Bernhard Mitchell
Australian Centre for Advanced Photovoltaics
School of Photovoltaic and Renewable Energy
University of New South Wales
Sydney, NSW 2052
Australia

Email: bernhard.mitchell@unsw.edu.au